

Class of Higgs-portal Dark Matter models in the light of gamma-ray excess from Galactic center

Tanushree Basak^a, Tanmoy Mondal^{a,b}

^aTheoretical Physics Division, Physical Research Laboratory, Ahmedabad 380009, India.

^bDepartment of Physics, Indian Institute of Technology, Gandhinagar, Ahmedabad, India.

Abstract

Recently the study of anomalous gamma-ray emission in the regions surrounding the galactic center has drawn a lot of attention as it points out that the excess of $\sim 1 - 3$ GeV gamma-ray in the low latitude is consistent with the emission expected from annihilating dark matter. The best-fit to the gamma-ray spectrum corresponds to dark matter (DM) candidate having mass in the range $\sim 31 - 40$ GeV annihilating into $b\bar{b}$ -pair with cross-section $\langle\sigma v\rangle = (1.4 - 2.0) \times 10^{-26} \text{ cm}^3\text{sec}^{-1}$. We have shown that the Higgs-portal dark matter models in presence of scalar resonance (in the annihilation channel) are well-suited for explaining these phenomena. In addition, the parameter space of these models also satisfy constraints from the LHC Higgs searches, relic abundance and direct detection experiments. We also comment on real singlet scalar Higgs-portal DM model which is found to be incompatible with the recent analysis.

Keywords: Dark matter phenomenology, Gamma-ray excess, Gauge extension of SM

1. Introduction

Gamma-ray emission from the galactic center (GC) and the inner galaxy regions as found in the Fermi-LAT data has gained a lot of attention from the perspective of dark matter (DM) searches. Past studies [1, 2, 3, 4, 5, 6, 7, 8] have pointed out a spatially extended excess of $\sim 1 - 3$ GeV gamma rays from the regions surrounding the galactic center, the morphology and spectrum of which is best fitted with that predicted from the annihilations of a $31 - 40$ GeV WIMP (weakly interacting massive particle) dark matter (DM) candidate annihilating mostly to b -quarks (or a $\sim 7 - 10$ GeV WIMP annihilating significantly to τ -leptons). Gamma rays from the galactic center is specially interesting because the region is predicted to contain very high densities of dark matter. Alternative explanations such as gamma-ray excess originating from thousands of unresolved millisecond pulsars have been disfavored since the signal extends well beyond the boundaries of the central stellar cluster. A more recent scrutiny of the morphology and spectrum of the anomalous gamma-ray emission in order to identify the origin has confirmed that the signal is very well fitted by a $31 - 40$ GeV dark matter particle annihilating to $b\bar{b}$ with an annihilation cross section of $\sigma v = (1.4 - 2.0) \times 10^{-26} \text{ cm}^3\text{sec}^{-1}$ (normalized to a local dark matter density of 0.3 GeV cm^{-3}) [9], which is accidentally close to the weak cross-section for producing correct relic abundance.

The excess seen in the gamma ray spectrum at the low latitude region can be well explained in a simple dark matter model, where the DM dominantly annihilates into quark pairs with cross-section in the desired range for obtaining correct relic abundance. Already a handful of particle physics model of dark matter [10, 11, 12, 13, 14, 15, 16, 17, 18, 19, 20, 21, 22, 23, 24, 25, 26, 27, 28, 29] have been proposed to explain the reported gamma-ray excess. Among these some are focused on various Higgs-portal dark matter models [11, 12, 20]. These kind of models are simply interesting because they enjoy a special feature of scalar resonances, provided dark matter mass is half of the scalar mass(es). This resonant feature is crucial as it enhances the annihilation cross-section.

In this letter, we have studied a class of Higgs-portal dark matter models to explain the reported excess. We showed that the simplest Higgs-portal model, i.e, the real singlet scalar extension of the Standard model (SM), is inconsistent with a $30 - 40$ GeV dark matter, because of the absence of resonance. Another Higgs-portal model considered in this letter is the so-called Singlet fermionic dark matter (SFDM) model, which consist of SM alongwith a hidden sector with a gauge singlet scalar and a Dirac-fermion singlet, acting as a potential DM candidate. We analyse the parameter space of this model owing to constraints from LHC bound on SM-Higgs, relic density and direct detection of DM. We found this model to be consistent as well with the requirements to explain the galactic center γ -ray excess. The last model we consider is the minimal $U(1)_{B-L}$ extension of the SM with a SM singlet scalar S and three right-handed (RH) neutrinos. The third generation RH-neutrino, which is a Majorana fermion, serves

Email addresses: tanu@prl.res.in (Tanushree Basak),
tanmoy@prl.res.in (Tanmoy Mondal)

as a viable DM candidate as an artifact of \mathbb{Z}_2 -symmetry. The parameters like DM coupling with the SM-Higgs boson and scalar mixing are subject to the constraints from the LHC Higgs searches apart from other observational constraints on dark matter. However, annihilation of Majorana fermionic dark matter through a scalar resonance is velocity suppressed. But, the presence of a very narrow scalar resonance in the DM annihilation channel lifts the cross sections considerably via Breit-Wigner enhancement at later times and makes the model compatible with the recent analysis.

2. Class of Higgs-portal dark matter models

The basic feature of Higgs-portal model is that all the interactions of DM are mediated through Higgs(es) and the presence of scalar resonance plays a crucial role in determining the correct relic abundance. Here, we will discuss a class of Higgs-portal DM model in the light of the recent analysis [9] of the excess gamma-ray emission in the Fermi-bubble.

2.1. Scalar Singlet extension of SM

The scalar singlet extension of SM [30, 31, 32, 33, 34, 35, 36] is the most simplified Higgs-portal model to account for a WIMP candidate. The real singlet S' , stabilized by odd \mathbb{Z}_2 -parity, acts as a viable DM candidate. It interacts only with the SM Higgs boson through the renormalizable interaction term present in the lagrangian,

$$\mathcal{L} = \mathcal{L}_{SM} + \frac{1}{2}(\partial S')^2 - \frac{1}{2}\mu_{S'}^2 S'^2 + \mathcal{L}_{int} - \lambda S'^4 \quad (1)$$

where, $\mathcal{L}_{int} = -\lambda_{S'}|\Phi|^2 S'^2$.

The mass of the DM after EWSB becomes, $m_{DM}^2 = \mu_{S'}^2 + \frac{1}{2}\lambda_{S'}v^2$. The coupling between DM and SM-Higgs, i.e, $\lambda_{S'}$ is constrained from the invisible decay width of Higgs boson when $m_{S'} \lesssim m_h/2$, such that $\text{BR}(h \rightarrow SS) \lesssim 0.20$ [37]. Figure. 1 shows the contours of invisible branching ratio of the SM Higgs boson in $\lambda_{S'} - m_{DM}$ plane. Region above red-dashed line is excluded as in the region the invisible branching ratio of the SM Higgs is more than 20%. Blue-solid, green-dotted and purple-dot-dashed contours show the allowed region if the invisible branching ratio is 25%, 30% and 35% respectively. As expected, the more invisible decay, the higher values of $\lambda_{S'}$ are allowed. For example, $\lambda_{S'}$ must be $\lesssim 8 \times 10^{-3}$ if 20% of the SM Higgs decays invisibly.

2.1.1. Relic Abundance

The relic abundance of DM can be formulated as [38],

$$\Omega_{CDM} h^2 = 1.1 \times 10^9 \frac{x_f}{\sqrt{g^*} m_{Pl} \langle \sigma v \rangle_{ann}} \text{GeV}^{-1}, \quad (2)$$

where $x_f = m_{DM}/T_D$ with T_D as decoupling temperature. m_{Pl} is Planck mass $= 1.22 \times 10^{19}$ GeV, and, g^* is effective number of relativistic degrees of freedom. $\langle \sigma v \rangle_{ann}$ is the

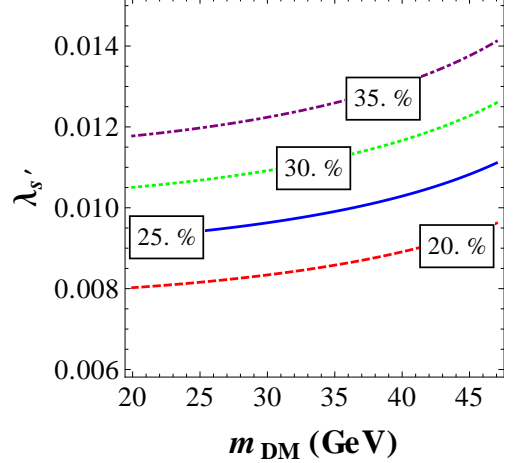


Figure 1: Contours of invisible branching ratio for singlet scalar DM model, in the plane of $\lambda_{S'} - m_{DM}$. Region above red-dashed (blue-solid, green-dotted and purple-dot-dashed) line is excluded if the SM Higgs has invisible branching ratio upto 20% (25%, 30% and 35%).

thermal averaged value of DM annihilation cross-section times relative velocity. $\langle \sigma v \rangle_{ann}$ can be obtained using the well known formula [39],

$$\langle \sigma v \rangle_{ann} = \frac{1}{m_{DM}^2} \left\{ w(s) - \frac{3}{2} \left(2w(s) - 4m_{DM}^2 w'(s) \right) \frac{1}{x_f} \right\}, \quad (3)$$

where prime denotes differentiation with respect to s (\sqrt{s} is the center of mass energy) and evaluated at $s = (2m_{DM})^2$. The function $w(s)$ is same as defined in [40].

In order to fit the spectrum of the gamma-ray emission near the galactic center, one requires a WIMP of mass $\sim 31 - 40$ GeV, which dominantly annihilates into final state $b\bar{b}$ through the s-channel exchange of the SM-Higgs boson. Also we choose, $\lambda_{S'} \simeq 0.007$ as a benchmark value. We obtain that $\langle \sigma v \rangle_{b\bar{b}} = (0.92 - 2.17) \times 10^{-30} \text{ cm}^3/\text{s}$, which cannot fit the observed gamma-ray signal. We also found that such a WIMP candidate cannot produce the required relic-abundance unless a scalar resonance is present i.e, when, $m_{S'} \simeq m_h/2 \sim 62$ GeV. Also Ref.[35] has mentioned that for $m_{S'} < m_h/2$, the parameter space is severely restricted from both LHC and direct detection constraints. We conclude that the singlet scalar DM with mass around 31-40 GeV is incompatible with the dark matter interpretation for the gamma ray excess from GC.

2.2. Singlet fermionic dark matter model

The singlet fermionic dark matter (SFDM) model is a renormalizable extension of SM with a hidden sector containing a scalar singlet Φ_s and a singlet Dirac fermion ψ [41, 42]. Here, the singlet fermionic dark matter ψ , interacts with the SM sector via the singlet Φ_s which mixes with the SM-Higgs doublet Φ . Therefore, this is also an example of Higgs-portal model. The lagrangian of the SFDM model is given as,

$$\mathcal{L} = \mathcal{L}_{SM} + \mathcal{L}_{hid} + \mathcal{L}_{int} \quad (4)$$

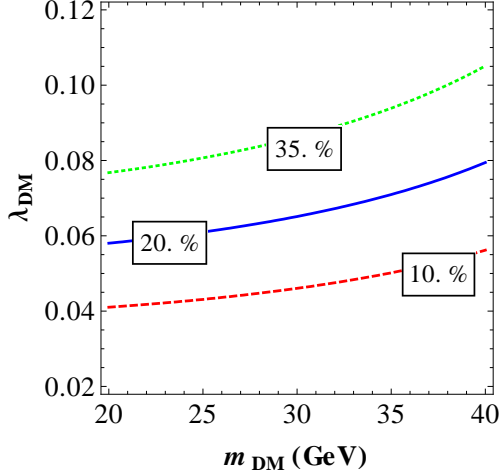


Figure 2: Contours of invisible branching ratio for SFDM model (10%, 20%, and 35%) in the plane of $[m_{DM}, \lambda_{DM}]$ with $\cos \alpha = 0.95$.

where,

$$\mathcal{L}_{hid} = \mathcal{L}_{\Phi_s} + \bar{\psi}(i\partial_\mu \gamma^\mu - m_\psi)\psi - \lambda_{\psi S} \bar{\psi}\psi\Phi_s \quad (5)$$

$$\mathcal{L}_{int} = \frac{\lambda'_1}{2} \Phi^\dagger \Phi \Phi_s + \frac{\lambda'_2}{2} \Phi^\dagger \Phi \Phi_s^2 \quad (6)$$

$$\mathcal{L}_{\Phi_s} = \frac{1}{2}(\partial\Phi_s)^2 - \frac{m_{\Phi_s}^2}{2}\Phi_s^2 - \frac{\lambda'}{3}\Phi_s^3 - \frac{\lambda''}{4}\Phi_s^4 \quad (7)$$

After EWSB, the singlet field Φ_s can be written as, $\Phi_s = x + s$, where x is the VEV of Φ_s and $\Phi = (0 \ v + \phi)^T$. The two scalar eigenstates are denoted as,

$$H_2 = \sin \alpha \ s + \cos \alpha \ \phi \quad (8)$$

$$H_1 = \sin \alpha \ \phi - \cos \alpha \ s \quad (9)$$

where, H_2 is identified as the SM-Higgs boson and we consider the case when, $m_{H_2} > m_{H_1}$. Now, the mass of the DM is given by, $m_{DM} = m_\psi + \lambda_{\psi S} x$, with m_ψ as a free parameter. In order to explain the observed gamma-ray excess in the low latitude, we consider the following set of parameters, $m_{DM} \sim 31$ GeV, $m_{H_1} \simeq 2m_{DM}$. The DM interaction strength depends on the parameter $\lambda_{DM} = \lambda_{\psi S}$. Thus, the two parameters λ_{DM} and scalar mixing $\cos \alpha$ play crucial role in DM phenomenology. Here, the scalar mixing angle and DM-coupling are subject to various constraints like LHC bound on SM-Higgs boson, relic abundance of DM and upper bound on the DM-nucleon scattering cross section.

2.2.1. Constraints from LHC

Observation of SM-like Higgs boson at LHC by CMS [43] and ATLAS [44] collaboration will constrain this mixing angle severely. The signal strength or reduction factor of a particular channel can be defined as:

$$r_i^{xx} = \frac{\sigma_{H_i}}{\sigma_{H_i}^{SM}} \cdot \frac{BR_{H_i \rightarrow xx}}{BR_{H_i \rightarrow xx}^{SM}}, \quad (i = 1, 2). \quad (10)$$

where, σ_{H_i} and $BR_{H_i \rightarrow xx}$ are the production cross section of H_i , and the branching ratio of $H_i \rightarrow xx$ respectively.

Similarly, $\sigma_{H_i}^{SM}$ and $BR_{H_i \rightarrow xx}^{SM}$ are the corresponding quantities of the SM-Higgs. Using eq. 10 one obtains,

$$r_2 = \cos^4 \alpha \frac{\Gamma_{H_2}^{SM}}{\cos^2 \alpha \Gamma_{H_2}^{SM} + \sin^2 \alpha \Gamma_{H_2}^{Hid} + \Gamma_{H_2 \rightarrow H_1 H_1}}$$

$$r_1 = \sin^4 \alpha \frac{\Gamma_{H_1}^{SM}}{\sin^2 \alpha \Gamma_{H_1}^{SM} + \cos^2 \alpha \Gamma_{H_1}^{Hid}} \quad (11)$$

where, $\Gamma_{H_i}^{SM}$ denotes the total decay width of the SM-Higgs boson and $\Gamma_{H_i}^{Hid}$ is the invisible decay width ($H_i \rightarrow 2$ DM). The invisible decay width of the SM Higgs reads as

$$\Gamma_{H_2}^{Hid} \equiv \Gamma_{inv} = \frac{m_{H_2} \lambda_{DM}^2}{16\pi} \sin^2 \alpha \left(1 - 4 \frac{m_{DM}^2}{m_{H_2}^2}\right)^{\frac{3}{2}}, \quad (12)$$

Since, $m_{DM} < m_{H_2}/2$, we can constrain the DM coupling λ_{DM} from the invisible decay width of SM-Higgs boson. Figure.2 shows the allowed range of λ_{DM} with mass of DM for different invisible branching ratio of the SM-Higgs boson, assuming the width of the Higgs to SM fermions as 4.21 MeV. We observe that for $m_{DM} \sim 30$ GeV, if $BR_{inv} \geq 20\%$ (35%) then DM-coupling, λ_{DM} should be less than 0.06 (0.075). Again, the signal strength (as defined in eqs. 10-11) depends on the scalar mixing angle. Constraining r_2 to be ≤ 0.9 (or 0.8), we obtain the allowed range of scalar mixing $\cos \alpha$ as a function of m_{DM} for a particular value of DM-coupling.

2.2.2. Constraints from relic density and direct detection

We obtain the relic abundance (using Eqn. 2) of the dark matter in agreement with WMAP-9 year result [45] and PLANCK [46], only near resonance where, $m_{DM} = m_{h_1}/2 \sim 31$ GeV. Dominant contribution to relic density comes from final-state $b\bar{b}$ annihilation with cross-section $\langle \sigma v \rangle \simeq 1.7 \times 10^{-26} \text{cm}^3 \text{sec}^{-1}$, which is also in the desired range for explaining galactic center γ -ray excess. We observe that as we decrease λ_{DM} , the annihilation cross-section is also decreased. But, if we approach very near the resonance region, i.e, $m_{H_1} - 2m_{DM} \sim \mathcal{O}(10^{-4})$, the annihilation cross-section can be enhanced significantly, which counter-balance the previous effect. However, if we are slightly away from resonance we need to have $\lambda_{DM} \sim 10^{-2}$, to get correct relic.

The scattering cross-section (spin-independent) for the dark matter off a proton or neutron as,

$$\sigma_{p,n}^{SI} = \frac{4m_r^2}{\pi} f_{p,n}^2 \quad (13)$$

where, m_r is the reduced mass defined as, $1/m_r = 1/m_{DM} + 1/m_{p,n}$ and $f_{p,n}$ is the hadronic matrix element, given by

$$f_{p,n} = \sum_{q=u,d,s} f_{Tq}^{(p,n)} a_q \frac{m_{p,n}}{m_q} + \frac{2}{27} f_{TG}^{(p,n)} \sum_{q=c,b,t} a_q \frac{m_{p,n}}{m_q}.$$

The f-values are given in [47]. Here, a_q is the effective coupling constant between the DM and the quark. An

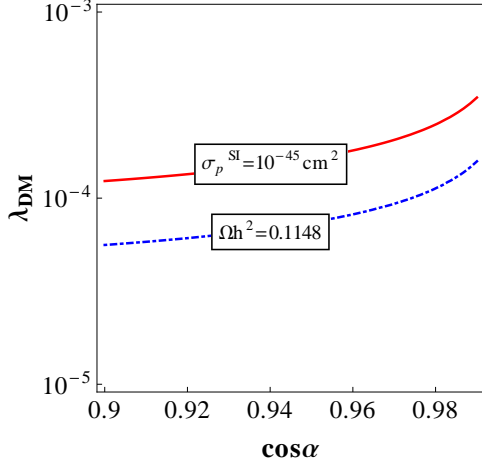


Figure 3: Contours of relic abundance (blue-dot-dashed) consistent with WMAP9 [45] and spin-independent scattering cross-sections for SFDM model, $\sigma_p^{SI} = 10^{-45} \text{cm}^2$ (red-solid), in the plane of $[\lambda_{DM}, \cos \alpha]$ for $m_{DM} \sim 31 \text{ GeV}$.

approximate form of a_q/m_q can be recast as :

$$\frac{a_q}{m_q} = \frac{\lambda_{DM}}{v\sqrt{2}} \left[\frac{1}{m_h^2} - \frac{1}{m_H^2} \right] \sin \alpha \cos \alpha. \quad (14)$$

In order to be consistent with the latest exclusion limit on σ_p^{SI} as specified by LUX [48], XENON 100 [49, 50], we require $\sigma_p^{SI} \lesssim 10^{-45} \text{cm}^2$. In Figure. 3, we show the contour of $\sigma_p^{SI} = 10^{-45} \text{cm}^2$ (red-solid). It indicates that λ_{DM} should be small enough (in the range of $\sim 10^{-4} - 10^{-5}$) to satisfy the required value of σ_p^{SI} . As argued before, very near resonance region, for $\lambda_{DM} \sim 10^{-4}$, also gives correct relic density. The contour of relic abundance has been shown in Figure. 3 by the blue-dot-dashed line.

2.3. Minimal $U(1)_{B-L}$ gauge extension of SM

The minimal $U(1)_{B-L}$ extension of the SM [51, 52, 53, 40] contains in addition to SM : a SM singlet S with $B-L$ charge $+2$, three right-handed neutrinos $N_R^i (i = 1, 2, 3)$ having $B-L$ charge -1 . The assignment of \mathbb{Z}_2 -odd charge ensures the stability of N_R^3 [54, 55] which qualified as a viable DM candidate. Scalar Lagrangian of this model can be written as,

$$\mathcal{L}_s = (D^\mu \Phi)^\dagger D_\mu \Phi + (D^\mu S)^\dagger D_\mu S - V(\Phi, S), \quad (15)$$

where the potential term is,

$$V(\Phi, S) = m^2 \Phi^\dagger \Phi + \mu^2 |S|^2 + \lambda_1 (\Phi^\dagger \Phi)^2 + \lambda_2 |S|^4 + \lambda_3 \Phi^\dagger \Phi |S|^2,$$

with Φ and S as the SM-scalar doublet and singlet fields, respectively. After spontaneous symmetry breaking (SSB) the singlet scalar field can be written as, $S = \frac{v_{B-L} + \phi'}{\sqrt{2}}$ with v_{B-L} real and positive. The mass eigenstates (H_1, H_2) are linear combinations of ϕ and ϕ' with mixing angle α . We identify H_2 as the SM-like Higgs boson with mass 125.5

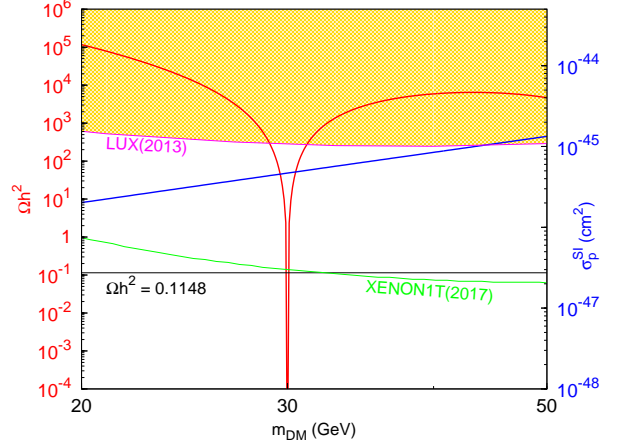


Figure 4: Shows the relic abundance (red curve) and scattering cross-section (blue curve) as a function of DM mass. The black (solid) line shows the latest 9-year WMAP data i.e. $\Omega_{CDM} h^2 = 0.1148 \pm 0.0019$ [45]. The yellow region above is excluded by LUX(2013) [48] and the green (dashed) line shows the projected sensitivity of XENON1T experiment [57].

GeV. We choose $v_{B-L} \simeq 4 \text{ TeV}$, in accordance with the constraint on the mass of Z' -boson [56].

The scalar mixing angle, α can be expressed as:

$$\tan(2\alpha) = \frac{\lambda_3 v_{B-L} v}{\lambda_1 v^2 - \lambda_2 v_{B-L}^2}. \quad (16)$$

The RH neutrinos interact with the singlet scalar field S through interaction term of the lagrangian:

$$\mathcal{L}_{int} = \sum_{i=1}^3 \frac{y_{n_i}}{2} \overline{N_R^i} S N_R^i. \quad (17)$$

Here we define, λ_{DM} as the coupling between DM candidate and the SM Higgs boson, which is effectively the Yukawa coupling of the N_R^3 . Thus, the mass of dark matter is given by, $m_{DM} = m_{N_R^3} = \frac{y_{n_3}}{\sqrt{2}} v_{B-L}$.

2.3.1. Constraints from LHC

As λ_{DM} is suppressed by $B-L$ symmetry breaking VEV, the invisible decay width remains very small ($\sim 0.5\%$) for DM mass $\sim 30 - 40 \text{ GeV}$.

On the other hand, the decay width of the SM Higgs decays to light scalar boson is

$$\Gamma_{H_2 \rightarrow H_1 H_1} = \frac{g_{H_2 H_1 H_1}^2}{32\pi m_{H_2}} \sqrt{1 - 4 \frac{m_{H_1}^2}{m_{H_2}^2}}. \quad (18)$$

where $g_{H_2 H_1 H_1}$ is defined in [40]. In order to have H_2 as a SM Higgs boson we require $r_2 \geq 0.9$ (0.8) and correspondingly $r_1 \leq 0.1$ (0.2). We have obtained that r_2 being ≥ 0.9 (0.8) restricts the choice of scalar mixing such that, $\cos \alpha \geq 0.96$ (0.94) for $m_{DM} \sim 31 \text{ GeV}$.

2.3.2. Velocity dependent cross-section and Breit-Wigner enhancement

In general the annihilation of Majorana fermionic DM into SM-fermion pairs through a scalar mediator is velocity suppressed. In that case the thermally averaged annihilation cross-section can be written as,

$$\langle\sigma v\rangle = a + bv^2, \text{ where } a, b \text{ are model dependent variables.}$$

The term a comes from s-channel s-wave process, where as, b has contributions from both s-wave and p-wave. The averaged velocity v can be expressed as, $v \sim \sqrt{3/x}$. Because of p-wave suppression, $\langle\sigma v\rangle$ at the time of freeze-out ($x_f \sim 20$) is different than that at the galactic halo ($x \sim 10^6$). However, $\langle\sigma v\rangle$ at the galactic halo can be substantially enhanced using the Breit-Wigner mechanism [58, 59], where the DM annihilates through a narrow s-channel resonance.

The leading annihilation channels of DM are, $N_R^3 N_R^3 \rightarrow b\bar{b}, \tau^+ \tau^-$. The s-channel resonant annihilation cross-section into final state $b\bar{b}$ (dominant) is given as,

$$\begin{aligned} 4E_1 E_2 \sigma v &= \frac{1}{8\pi} \sqrt{1 - \frac{4m_b^2}{s}} |\bar{M}|^2 \\ &= \frac{\lambda_{DM}^2 \cos^2 \alpha}{32\pi^2} \frac{s^2}{m_{H_1}^2} \frac{m_{H_1} \Gamma_{H_1}}{(s - m_{H_1}^2)^2 + m_{H_1}^2 \Gamma_{H_1}^2} \end{aligned}$$

where, Γ_{H_1} is the total decay width of H_1 .

Here, we introduce two parameters δ and γ as,

$$m_{H_1}^2 = 4m_{DM}^2(1 - \delta), \quad \gamma = \Gamma_{H_1}/m_{H_1}. \quad (19)$$

Clearly, $\delta < 0$ and $\delta > 0$ represents the physical and unphysical pole respectively. Adopting the single-integral formula for thermally averaged cross-section, we obtain,

$$\begin{aligned} \langle\sigma v\rangle &= \frac{1}{n_{EQ}^2} \frac{m_{DM}}{64\pi^4 x} \int_{4m_{DM}^2}^{\infty} ds \, 4E_1 E_2 \sigma v \sqrt{s} g_i^2 \\ &\times \sqrt{1 - \frac{4m_{DM}^2}{s}} K_1\left(\frac{x\sqrt{s}}{m_{DM}}\right) \end{aligned} \quad (20)$$

where,

$$n_{EQ} = \frac{g_i}{2\pi^2} \frac{m_{DM}^3}{x} K_2(x)$$

$K_1(x)$ and $K_2(x)$ are the modified Bessel's function of second kind and g_i is the internal degrees of freedom of dark matter particle.

We again redefine s as, $s = 4m_{DM}^2(1 + y)$ where, $y \propto v^2$. Eq.20 can be recast in terms of δ , γ and y as,

$$\langle\sigma v\rangle \propto x^{3/2} \int_0^{y_{eff}} \frac{\sqrt{y}(1+y)^{3/2} e^{-xy}}{(y+\delta)^2 + \gamma^2(1-\delta^2)} dy \quad (21)$$

where, $y_{eff} \sim \max[4/x, 2|\delta|]$ for $\delta < 0$ and $y_{eff} \sim 4/x$ for $\delta > 0$ case. If δ and γ are much smaller than unity, $\langle\sigma v\rangle$ scales as v^{-4} in the limit $v^2 \gg \max[\gamma, \delta]$. At smaller velocity, the thermally averaged annihilation cross-section

becomes proportional to v^{-2} and approach towards a constant value when $v^2 \ll \max[\gamma, \delta]$.

We obtain the relic abundance using eqs.(2,20). Fig.4 shows the relic abundance (red curve) as a function of DM mass. The resultant relic abundance is found to be consistent with the reported value of WMAP-9 [45] (shown by the black solid line) and PLANCK experiment [46], only near resonance when, $m_{DM} \sim (1/2) m_{H_1}$.

We have also achieved the required $\langle\sigma v\rangle_{b\bar{b}} \sim 1.881 \times 10^{-26} \text{ cm}^3/\text{s}$ at the galactic halo through the Breit-Wigner enhancement given the value of parameters¹ $\delta \simeq -10^{-3}$ and $\gamma \simeq 10^{-5}$. Note that, the same set of parameter values have been used to compute the relic abundance.

2.3.3. Constraints from direct detection searches

The spin-independent scattering cross-section of DM off nucleon is obtained using eq.13. In Fig.4 the yellow region above is excluded by LUX(2013) [48]. We observe that the resultant spin-independent scattering cross-section (blue curve) lies well below the LUX exclusion limit. However, the projected sensitivity of XENON1T experiment [57] (green-dashed line) might constrain the scenario of $m_{DM} = 31 - 40 \text{ GeV}$ in this model.

3. Summary and Conclusion

The excess of γ -ray emission in the low latitude region near the galactic center can be explained by annihilation of DM (in the mass range $\sim 31 - 40 \text{ GeV}$) into $b\bar{b}$, with cross-section of the order of the weak cross-section (i.e $\sim 10^{-26} \text{ cm}^3 \text{ sec}^{-1}$). In this context, we have analysed a class of Higgs-portal DM models and constrain the parameter space of these models. We found that the real singlet scalar DM model is incompatible with the recent analysis. However, the singlet fermionic dark matter model can account for this phenomena apart from satisfying relic abundance criterion. Besides this, the SI-scattering cross-section can be well below the exclusion limit from LUX, XENON 100, provided λ_{DM} lies below $\sim 10^{-4}$. Also, RH-neutrino DM in the minimal $U(1)_{B-L}$ model is well-suited for explaining the galactic-center gamma-ray excess along with satisfying other DM and collider constraints. The relic abundance is found to be consistent with the recent WMAP9 and PLANCK data only near scalar resonances, i.e, $m_{DM} \simeq m_{H_1}/2$. Here, we obtain the required $\langle\sigma v\rangle$ for explaining this reported excess at the galactic center through Breit-Wigner enhancement mechanism. Although, future experiment like XENON 1T can further restrict the parameter space of minimal $U(1)_{B-L}$ model.

In passing by, we would like to mention that the anti-proton data from indirect detection experiments like PAMELA [60, 61], AMS-02 [62] have constrained the annihilation cross-section into hadronic (mostly $b\bar{b}$) final states

¹Also for positive values of δ (for example, $\delta \simeq 10^{-1}$ and $\gamma \simeq 10^{-5}$), it is possible to obtain the required boost factor [58, 59]

in a model independently way. But, the present exclusion limit on $\langle\sigma v\rangle_{b\bar{b}}$ lies much above the reported value in Ref.[9] for DM mass in the range 31-40 GeV. However, the bound on $\langle\sigma v\rangle_{b\bar{b}}$ from the projected anti-proton data of AMS-02 (see Fig.1 of Ref.[22]) can be an important discriminator of dark matter models.

Acknowledgements

We would like to thank Partha Konar and Subhendra Mohanty for most useful comments and discussions.

- [1] L. Goodenough and D. Hooper (2009), 0910.2998.
- [2] A. Boyarsky, D. Malyshev, and O. Ruchayskiy, Phys.Lett. **B705**, 165 (2011), 1012.5839.
- [3] D. Hooper and L. Goodenough, Phys.Lett. **B697**, 412 (2011), 1010.2752.
- [4] D. Hooper and T. Linden, Phys.Rev. **D84**, 123005 (2011), 1110.0006.
- [5] K. N. Abazajian and M. Kaplinghat, Phys.Rev. **D86**, 083511 (2012), 1207.6047.
- [6] C. Gordon and O. Macias, Phys.Rev. **D88**, 083521 (2013), 1306.5725.
- [7] D. Hooper and T. R. Slatyer, Phys.Dark Univ. **2**, 118 (2013), 1302.6589.
- [8] K. N. Abazajian, N. Canac, S. Horiuchi, and M. Kaplinghat (2014), 1402.4090.
- [9] T. Daylan, D. P. Finkbeiner, D. Hooper, T. Linden, S. K. N. Portillo, et al. (2014), 1402.6703.
- [10] W.-C. Huang, A. Urbano, and W. Xue (2013), 1310.7609.
- [11] K. P. Modak, D. Majumdar, and S. Rakshit (2013), 1312.7488.
- [12] N. Okada and O. Seto, Phys.Rev. **D89**, 043525 (2014), 1310.5991.
- [13] K. Hagiwara, S. Mukhopadhyay, and J. Nakamura, Phys.Rev. **D89**, 015023 (2014), 1308.6738.
- [14] A. Martin, J. Shelton, and J. Unwin (2014), 1405.0272.
- [15] D. K. Ghosh, S. Mondal, and I. Saha (2014), 1405.0206.
- [16] C. Boehm, M. J. Dolan, C. McCabe, M. Spannowsky, and C. J. Wallace (2014), 1401.6458.
- [17] A. Berlin, D. Hooper, and S. D. McDermott (2014), 1404.0022.
- [18] P. Agrawal, B. Batell, D. Hooper, and T. Lin (2014), 1404.1373.
- [19] D. Cerdeno, M. Peiro, and S. Robles (2014), 1404.2572.
- [20] P. Ko, W.-I. Park, and Y. Tang (2014), 1404.5257.
- [21] S. Ipek, D. McKeen, and A. E. Nelson (2014), 1404.3716.
- [22] K. Kong and J.-C. Park (2014), 1404.3741.
- [23] B. Kyae and J.-C. Park, Phys.Lett. **B732**, 373 (2014), 1310.2284.
- [24] L. A. Anchordoqui and B. J. Vlcek, Phys.Rev. **D88**, 043513 (2013), 1305.4625.
- [25] E. Izaguirre, G. Krnjaic, and B. Shuve (2014), 1404.2018.
- [26] M. Abdullah, A. DiFranzo, A. Rajaraman, T. M. P. Tait, P. Tanedo, et al. (2014), 1404.6528.
- [27] C. Boehm, M. J. Dolan, and C. McCabe (2014), 1404.4977.
- [28] A. Alves, S. Profumo, F. S. Queiroz, and W. Shepherd (2014), 1403.5027.
- [29] D. Hooper, C. Kelso, and F. S. Queiroz, Astroparticle Physics **46**, 55 (2013), 1209.3015.
- [30] J. McDonald, Phys.Rev. **D50**, 3637 (1994), hep-ph/0702143.
- [31] C. Burgess, M. Pospelov, and T. ter Veldhuis, Nucl.Phys. **B619**, 709 (2001), hep-ph/0011335.
- [32] H. Davoudiasl, R. Kitano, T. Li, and H. Murayama, Phys.Lett. **B609**, 117 (2005), hep-ph/0405097.
- [33] A. Bandyopadhyay, S. Chakraborty, A. Ghosal, and D. Majumdar, JHEP **1011**, 065 (2010), 1003.0809.
- [34] W.-L. Guo and Y.-L. Wu, JHEP **1010**, 083 (2010), 1006.2518.
- [35] X.-G. He, B. Ren, and J. Tandean, Phys.Rev. **D85**, 093019 (2012), 1112.6364.
- [36] J. M. Cline, K. Kainulainen, P. Scott, and C. Weniger (2013), 1306.4710.
- [37] G. Belanger, B. Dumont, U. Ellwanger, J. Gunion, and S. Kraml, Phys.Lett. **B723**, 340 (2013), 1302.5694.
- [38] E. W. Kolb and M. S. Turner, Front.Phys. **69**, 1 (1990).
- [39] M. Srednicki, R. Watkins, and K. A. Olive, Nucl.Phys. **B310**, 693 (1988).
- [40] J. Chakraborty, P. Konar, and T. Mondal, Phys.Rev. **D89**, 056014 (2014), 1308.1291.
- [41] Y. G. Kim, K. Y. Lee, and S. Shin, JHEP **0805**, 100 (2008), 0803.2932.
- [42] S. Baek, P. Ko, W.-I. Park, and E. Senaha, JHEP **1211**, 116 (2012), 1209.4163.
- [43] S. Chatrchyan et al. (CMS Collaboration), Phys.Lett. **B716**, 30 (2012), 1207.7235.
- [44] G. Aad et al. (ATLAS Collaboration), Phys.Lett. **B716**, 1 (2012), 1207.7214.
- [45] G. Hinshaw et al. (WMAP Collaboration) (2012), 1212.5226.
- [46] P. Ade et al. (Planck Collaboration) (2013), 1303.5076.
- [47] J. R. Ellis, A. Ferstl, and K. A. Olive, Phys.Lett. **B481**, 304 (2000), hep-ph/0001005.
- [48] D. Akerib et al. (LUX Collaboration) (2013), 1310.8214.
- [49] L. S. Lavina (Collaboration XENON100), 1305.0224 (2013).
- [50] E. Aprile et al. (XENON100 Collaboration), Phys.Rev.Lett. **109**, 181301 (2012), 1207.5988.
- [51] S. Khalil, J.Phys. **G35**, 055001 (2008), hep-ph/0611205.
- [52] L. Basso, S. Moretti, and G. M. Pruna, Phys.Rev. **D82**, 055018 (2010), 1004.3039.
- [53] L. Basso (2011), 1106.4462.
- [54] N. Okada and O. Seto, Phys.Rev. **D82**, 023507 (2010), 1002.2525.
- [55] T. Basak and T. Mondal, Phys.Rev. **D89**, 063527 (2014), 1308.0023.
- [56] J. Beringer et al. (Particle Data Group), Phys. Rev. D **86**, 010001 (2012), URL <http://link.aps.org/doi/10.1103/PhysRevD.86.010001>.
- [57] E. Aprile (XENON1T collaboration) (2012), 1206.6288.
- [58] M. Ibe, H. Murayama, and T. Yanagida, Phys.Rev. **D79**, 095009 (2009), 0812.0072.
- [59] W.-L. Guo and Y.-L. Wu, Phys.Rev. **D79**, 055012 (2009), 0901.1450.
- [60] O. Adriani, G. C. Barbarino, G. A. Bazilevskaya, R. Bellotti, M. Boezio, E. A. Bogomolov, L. Bonechi, M. Bongi, V. Bonvicini, S. Borisov, et al., Physical Review Letters **105**, 121101 (2010), 1007.0821.
- [61] M. Cirelli and G. Giesen, JCAP **1304**, 015 (2013), 1301.7079.
- [62] M. Aguilar et al. (AMS Collaboration), Phys.Rev.Lett. **110**, 141102 (2013).